



# Temperatures from Energy Balance Models: the effective heat capacity matters

Gerrit Lohmann<sup>1,2</sup>

<sup>1</sup> Alfred Wegener Institute, Helmholtz Centre for Polar and Marine Research, Bremerhaven, Germany

<sup>2</sup> University of Bremen, Bremen, Germany

**Correspondence:** Gerrit Lohmann (Gerrit.Lohmann@awi.de)

**Abstract.** Energy balance models (EBM) are highly simplified systems of the climate system. The global temperature is calculated by the radiation budget through the incoming energy from the Sun and the outgoing energy from the Earth. The argument that the temperature can be calculated by the simple radiation budget is revisited. The underlying assumption for a realistic temperature distribution is explored: One has to assume a moderate diurnal cycle due to the large heat capacity and the fast rotation of the Earth. Interestingly, the global mean in the revised EBM is very close to the originally proposed value. The time dependent-EBM predicts a flat meridional temperature gradient for large heat capacities which can be related to very effective vertical diffusion. Motivated by this finding, sensitivity experiments with a complex model are performed where the vertical diffusion in the ocean has been increased. The resulting climate shows a flat meridional temperature gradient and a deeper thermocline. The common pattern of surface temperature anomalies and climate reconstructions suggests a possible mechanism for past climate changes prior to 3 million years ago.

**Keywords.** Energy balance model, Earth system modeling, Temperature gradient, Climate change, Climate sensitivity, Climate reconstructions

## 1 Introduction

Energy balance models (EBMs) are among the simplest climate models. They were introduced almost simultaneously by Budyko (1969) and Sellers (1969). Because of their simplicity, these models are easy to understand and facilitate both analytical and numerical studies of climate sensitivity (Peixoto and Oort, 1992; Hartmann, 1994; Saltzman, 2001; Ruddiman, 2001; Pierrehumbert, 2010). A key feature of these models is that they eliminate the climate's dependence on the wind field, ocean currents, the Earth rotation, and thus have only one dependent variable: the Earth's near-surface air temperature  $T$ .

With the development of computer capacities, simpler models have not disappeared; on the contrary, a stronger emphasis has been given to the concept of a hierarchy of models' as the only way to provide a linkage between theoretical understanding and the complexity of realistic models (von Storch et al. 1999; Claussen et al. 2002). In contrast, many important scientific debates in recent years have had their origin in the use of conceptually simple models (Le Treut et al., 2007; Stocker, 2011), also as a way to analyze data (Köhler et al., 2010) or complex models (Knorr et al., 2011).



Pioneering work has been done by North (North, 1975a, b; 1981; 1983) and these models were applied subsequently (e.g., Ghil, 1976; Su and Hsieh, 1976; Ghil and Childress, 1987; Short et al., 1991; Stocker et al., 1992). Later the EMBs were equipped by the hydrological cycle (Chen et al., 1995; Lohmann et al., 1996; Fanning and Weaver, 1996; Lohmann and Gerdes, 1998) to study the feedbacks in the atmosphere-ocean-sea ice system. One of the most useful examples of a simple, but powerful, model is the one-/zero-dimensional energy balance model. As a starting point, a zero-dimensional model of the radiative equilibrium of the Earth is introduced (Fig. 1)

$$(1 - \alpha)S\pi R^2 = 4\pi R^2\epsilon\sigma T^4 \quad (1)$$

where the left hand side represents the incoming energy from the Sun (size of the disk= shadow area  $\pi R^2$ ) while the right hand side represents the outgoing energy from the Earth (Fig. 1). T is calculated from the Stefan-Boltzmann law assuming a constant radiative temperature, S is the solar constant - the incoming solar radiation per unit area- about  $1367 \text{ W m}^{-2}$ ,  $\alpha$  is the Earth's average planetary albedo, measured to be 0.3. R is Earth's radius =  $6.371 \times 10^6$  m,  $\sigma$  is the Stefan-Boltzmann constant =  $5.67 \times 10^{-8} \text{ JK}^{-4} \text{ m}^{-2} \text{ s}^{-1}$ , and  $\epsilon$  is the effective emissivity of Earth (about 0.612) (e.g., Archer 2010). The geometrical constant  $\pi R^2$  can be factored out, giving

$$(1 - \alpha)S = 4\epsilon\sigma T^4 \quad (2)$$

Solving for the temperature,

$$T = \sqrt[4]{\frac{(1 - \alpha)S}{4\epsilon\sigma}} \quad (3)$$

Since the use of the effective emissivity  $\epsilon$  in (1) already accounts for the greenhouse effect we gain an average Earth temperature of 288 K ( $15^\circ\text{C}$ ), very close to the global temperature observations/reconstructions (Hansen et al., 2011) at  $14^\circ\text{C}$  for 1951-1980. Interestingly, (3) does not contain parameters like the heat capacity of the planet. We will explore that this is essential for the temperature of the Earth's climate system.

## 2 A closer look onto the spatial distribution

Let us have a closer look onto (1). The local radiative equilibrium of the Earth is

$$\epsilon\sigma T^4 = (1 - \alpha)S \cos\varphi \cos\Theta \times 1_{[-\pi/2 < \Theta < \pi/2]}(\Theta) \quad (4)$$

where  $\varphi$  and  $\Theta$  are the latitude and longitude, respectively. Integration over the Earth surface is

$$\begin{aligned} \int_{-\pi/2}^{\pi/2} \left( \int_0^{2\pi} \epsilon\sigma T^4 R \cos\varphi d\Theta \right) R d\varphi &= (1 - \alpha)S \int_{-\pi/2}^{\pi/2} R \cos^2\varphi d\varphi \cdot \int_{-\pi/2}^{\pi/2} R \cos\Theta d\Theta \\ \epsilon\sigma R^2 \frac{4\pi}{4\pi} \int_{-\pi/2}^{\pi/2} \left( \int_0^{2\pi} T^4 \cos\varphi d\Theta \right) d\varphi &= (1 - \alpha)S R^2 \underbrace{\int_{-\pi/2}^{\pi/2} \cos^2\varphi d\varphi}_{\frac{\pi}{2}} \cdot \underbrace{\int_{-\pi/2}^{\pi/2} \cos\Theta d\Theta}_2 \\ \epsilon\sigma 4\pi \overline{T^4} &= (1 - \alpha)S \pi \end{aligned} \quad (5)$$



giving a similar formula as (3) with the definition for the average  $\overline{T^4}$ .

What we really want is the mean of the temperature  $\overline{T}$ . Therefore, we take the fourth root of (4):

$$T = \sqrt[4]{\frac{(1-\alpha)S \cos \varphi \cos \Theta}{\epsilon \sigma}} \times 1_{[-\pi/2 < \Theta < \pi/2]}(\Theta) \quad (6)$$

If we calculate the zonal mean of (6) by integration at the latitudinal cycles we have

$$\begin{aligned} 5 \quad T(\varphi) &= \frac{1}{2\pi} \int_{-\pi/2}^{-\pi/2} \sqrt[4]{\frac{(1-\alpha)S \cos \varphi \cos \Theta}{\epsilon \sigma}} d\Theta \\ &= \frac{\sqrt{2}}{2\pi} \underbrace{\int_{-\pi/2}^{\pi/2} (\cos \Theta)^{1/4} d\Theta}_{2.700} \sqrt[4]{\frac{(1-\alpha)S}{4\epsilon \sigma}} (\cos \varphi)^{1/4} \\ &= 0.608 \cdot \sqrt[4]{\frac{(1-\alpha)S}{4\epsilon \sigma}} (\cos \varphi)^{1/4} \end{aligned} \quad (7)$$

as a function on latitude (Fig. 2). When we integrate this over the latitudes, we obtain

$$\begin{aligned} 10 \quad \overline{T} &= \frac{1}{2} \int_{-\pi/2}^{\pi/2} T(\varphi) \cos \varphi d\varphi \\ &= \frac{0.608}{2} \cdot \sqrt[4]{\frac{(1-\alpha)S}{4\epsilon \sigma}} \underbrace{\int_{-\pi/2}^{\pi/2} (\cos \varphi)^{5/4} d\varphi}_{1.862} \\ &= 0.4\sqrt{2} \sqrt[4]{\frac{(1-\alpha)S}{4\epsilon \sigma}} = 0.566 \sqrt[4]{\frac{(1-\alpha)S}{4\epsilon \sigma}} \end{aligned} \quad (8)$$

Therefore,  $\overline{T} = 163\text{K}$  is a factor 0.566 lower than 288 K as stated at (1). The standard EBM in Fig. 1 has imprinted into our thoughts and lectures. We should therefore be careful and pinpoint the reasons for the failure.

15 What happens here is that the heat capacity of the Earth is neglected. During night, the temperature is very low and there is a strong non-linearity of the outgoing radiation. Furthermore, the Earth is a rapidly rotating object. Equation (6) can be better used for objects like the Moon or Mercury (Vasavada et al., 1999) as slowly rotating bodies without significant heat capacity.

### 3 The heat capacity and fast rotating body

The energy balance shall take the heat capacity into account:

$$C_p \partial_t T = (1-\alpha)S \cos \varphi \cos \Theta \times 1_{[-\pi/2 < \Theta < \pi/2]}(\Theta) - \epsilon \sigma T^4 \quad (9)$$

with  $C_p$  representing the heat capacity multiplied with the depth of the atmosphere-ocean layer ( $C_p$  is in the order of  $10^7 - 10^8 \text{ J K}^{-1} \text{ m}^{-2}$ ). If we consider the zonal mean and averaged over the diurnal cycle, we can assume that the heat capacity is



mainly given by the ocean. Observational evidence is that the diurnal variation of the ocean surface is in the order of 0.5-3 K with highest values at favorable conditions of high insolation and low winds (Stommel, 1969; Anderson et al., 1996; Kawai and Kawamura, 2002; Stuart-Menteth, et al. 2003; Ward, 2006). A significant heat capacity damping the surface temperatures are furthermore found over ice and soil. The atmospheric circulation provides an efficient way to propagate heat along latitudes which is ignored and is a second order effect (not shown). The energy balance (9) is integrated over the longitude and over the day

$$\tilde{T}(\tilde{t}) = \frac{1}{2\pi} \int_0^{2\pi} T(t) d\Theta \quad \text{with} \quad \tilde{T}^4 \approx \frac{1}{2\pi} \int_0^{2\pi} T^4 d\Theta$$

and therefore

$$\begin{aligned} C_p \partial_{\tilde{t}} \tilde{T} &= (1-\alpha) S \cos \varphi \cdot \underbrace{\frac{1}{2\pi} \int_{-\pi/2}^{\pi/2} \cos \Theta d\Theta}_2 - \epsilon \sigma \tilde{T}^4 \\ &= (1-\alpha) \frac{S}{\pi} \cos \varphi - \epsilon \sigma \tilde{T}^4 \end{aligned} \quad (10)$$

giving the equilibrium solution

$$5 \quad \tilde{T}(\varphi) = \sqrt[4]{\frac{4}{\pi}} \cdot \sqrt[4]{\frac{(1-\alpha)S}{4\epsilon\sigma}} (\cos \varphi)^{1/4} \quad (11)$$

shown in Fig. 2 as the read line with the mean

$$\begin{aligned} \bar{\tilde{T}} &= \sqrt[4]{\frac{4}{\pi}} \cdot \sqrt[4]{\frac{(1-\alpha)S}{4\epsilon\sigma}} \underbrace{\frac{1}{2} \int_{-\pi/2}^{\pi/2} (\cos \varphi)^{5/4} d\varphi}_{1.862} \\ &= \sqrt[4]{\frac{4}{\pi} \frac{1.862}{2}} \cdot \sqrt[4]{\frac{(1-\alpha)S}{4\epsilon\sigma}} = 0.989 \sqrt[4]{\frac{(1-\alpha)S}{4\epsilon\sigma}} \end{aligned} \quad (12)$$

Therefore,  $\bar{\tilde{T}} = 285 \approx 288$  K, very similar as in (1). A numerical solution of (9) is shown as the brownish dashed line in Fig. 2 where the diurnal cycle has been taken into account and  $C_p = C_p^a$  has been chosen as the atmospheric heat capacity

$$C_p^a = c_p p_s / g = 1004 \text{ JK}^{-1} \text{ kg}^{-1} \cdot 10^5 \text{ Pa} / (9.81 \text{ ms}^{-2}) = 1.02 \cdot 10^7 \text{ JK}^{-1} \text{ m}^{-2}$$

10 which is the specific heat at constant pressure  $c_p$  times the total mass  $p_s/g$ .  $p_s$  is the surface pressure and  $g$  the gravity. The temperature  $\bar{\tilde{T}}$  is 286 K, again close to 288 K.

The effect of heat capacity is systematically analyzed in Fig. 3. The temperatures are relative insensitive for a wide range of  $C_p$ . We find a severe drop in temperatures for heat capacities below 0.01 of the atmospheric heat capacity  $C_p^a$ . We find furthermore a pronounced temperature drop during night for low values of heat capacities and for long days (e.g. 240 h instead of 24 h) affecting the zonal temperatures (4.5 K colder at the equator). It is an interesting thought experiment what  
 15 would happen if the length of the daylight/night would change. The analysis shows that the effective heat capacity is of



great importance for the temperature, this depends on the atmospheric planetary boundary layer (how well-mixed with small gradients in the vertical) and the depth of the mixed layer in the ocean. To make a rough estimate of the involved mixed layer, one can see that the effective heat capacity of the ocean is time-scale dependent. A diffusive heat flux goes down the gradient of temperature and the convergence of this heat flux drives a ocean temperature tendency:

$$5 \quad C_p^o \partial_t T = -\partial_z(k^o \partial_z T) \quad (13)$$

where  $k_v = k^o / C_p^o$  is the oceanic vertical eddy diffusivity in  $m^2 s^{-1}$ , and  $C_p^o$  the oceanic heat capacity relevant on the specific time scale. The vertical eddy diffusivity  $k_v$  can be estimated from climatological hydrographic data (Olbers et al., 1985; Munk and Wunsch, 1998) and varies roughly between  $10^{-5}$  and  $10^{-4} m^2 s^{-1}$  depending on depth and region. A scale analysis of (13) yields a characteristic depth scale  $h_T$  through

$$10 \quad \frac{\Delta T}{\Delta t} = k_v \frac{\Delta T}{h_T^2} \quad \longrightarrow \quad h_T = \sqrt{k_v \Delta t} \quad (14)$$

For the diurnal cycle  $h_T$  is less than half a meter and the heat capacity generally less than that of the atmosphere. As pointed out by Schwartz (2007), the effective heat capacity that reflects only that portion of the global heat capacity that is coupled to the perturbation on the timescale of the perturbation. We discuss the sensitivity of the system with respect to  $k_v$  later in the context of a full circulation model.

#### 15 4 Meridional temperature gradients

Equation (10) shall be the starting point for further investigations. One can easily include the meridional heat transport by diffusion which has been previously used in one-dimensional EBMs (e.g. Adem, 1965; Sellers, 1969; Budyko, 1969; North, 1975a,b). In the following we will drop the tilde sign. Using a diffusion coefficient  $k$ , the meridional heat transport across a latitude is  $HT = -k \nabla T$ . One can solve the EBM

$$20 \quad C_p \partial_t T = \nabla \cdot HT + (1 - \alpha) \frac{S}{\pi} \cos \varphi - \epsilon \sigma T^4 \quad (15)$$

numerically. The boundary condition is that the HT at the poles vanish. The values of  $k$  are in the range of earlier studies (North, 1975a,b; Stocker et al., 1992; Chen et al., 1995; Lohmann et al., 1996). Fig. 4 shows the equilibrium solutions of (15) using different values of  $k$  (solid lines). The global mean temperature is not affected by the transport term because of the boundary condition with zero heat transport at the poles. The same is true if we introduce zonal transports because of the cyclic boundary condition in  $\theta$ -direction.

Until now, we assumed that the Earth's axis of rotation were vertical with respect to the path of its orbit around the Sun. Instead Earth's axis is tilted off vertical by about 23.5 degrees. As the Earth orbits the Sun, the tilt causes one hemisphere to receive more direct sunlight and to have longer days. This is a redistribution of heat with more solar insolation at the poles and less at the equator (formally it could be associated to an enhanced meridional heat transport HT). The resulting temperature is shown as the dotted blue line in Fig. 4. A spatially constant temperature in (1) can be formally seen as a system with infinite diffusion coefficient  $k \rightarrow \infty$  (black line in Fig. 4).



The global mean temperatures are not affected by the tilt and the values are identical to the one calculated in (12). This is true even if we calculate the seasonal cycle (Berger and Loutre 1991; 1997; Laepple and Lohmann 2009). However, if we include non-linearities such as the ice-albedo feedback ( $\alpha$  as a function of  $T$ ), the global mean value is changing (Budyko, 1969; Sellers, 1969; North et al., 1975a, b), cf. the dashed blue line in Fig. 4. Such model can be improved by including an explicit spatial pattern with a seasonal cycle to study the long-term effects of climate to external forcing (Adem, 1981; North et al., 1983) or by adding noise mimicking the effect of short-term features on the long-term climate (Hasselmann, 1976; Lemke, 1977; Lohmann, 2018).

As a logical next step, let us now include an explicit seasonal cycle into the EBM:

$$C_p \partial_t T = \nabla \cdot HT + (1 - \alpha)S(\varphi, t) - \epsilon\sigma T^4 \quad (16)$$

with  $S(\varphi, t)$  being calculated daily (Berger and Loutre, 1991; 1997). Eq. (16) is calculated numerically for fixed diffusion coefficient  $k = 1.5 \cdot 10^6 m^2/s$  under present orbital conditions. Fig. 5 indicates that the temperature gradient is getting flatter for large heat capacities. Furthermore, the mean temperature is affected by the choice of  $C_p$ . In the case of large heat capacity at high latitudes (for latitudes polewards of  $\varphi = 50^\circ$ ) and moderate elsewhere, we observe strong warming at high latitudes with moderate warming at low latitudes (dashed curve). This again indicates that we cannot neglect the time-dependent left hand side in the energy balance equations, both for the diurnal (9) as well as the seasonal (16) cycle for the temperature budget. In both considered cases, at strong diurnal/seasonal amplitude lowers the annual mean temperature. Fig. 6 shows the seasonal amplitude for the  $C_p$ -scenarios as indicated by the blue and dashed black lines, respectively. A change in the seasonal/diurnal cycle of  $T_1 - T_2 = 50^\circ C$  is equivalent to about  $10 W m^{-2}$  when applying the long wave radiation change  $\epsilon\sigma \cdot 0.5(T_1^4 + T_2^4) - \epsilon\sigma \cdot (0.5 \cdot (T_1 + T_2))^4$  for typical temperatures on the Earth. Please note that the number  $10 W m^{-2}$  is equivalent to a greenhouse gas forcing of more than quadrupling the  $CO_2$  concentration in the atmosphere.

## 5 Meridional temperature gradient in a complex model

Energy balance models have been used to diagnose the temperatures on the Earth when applying complex circulation models (e.g., Knorr et al. 2011) or data (e.g., Köhler et al., 2010; van der Heydt et al., 2016; Stap et al., 2018). For the past, a strong warming at high latitudes is reconstructed for the Pliocene, Miocene, Eocene periods (Markwick, 1994; Wolfe, 1994; Sloan and Rea, 1996; Huber et al., 2000; Shellito et al., 2003; Tripathi et al., 2003; Mosbrugger et al., 2005; Utescher and Mosbrugger, 2007). In the following this period is called Paleogene/Neogene, which covers the period  $3 \cdot 10^6 - 65 \cdot 10^6$  years ago. Until now, it is a conundrum that the modelled high latitudes are not as warm as the reconstructions (e.g., Sloan and Rea, 1996; Huber et al., 2000; Mosbrugger et al., 2005; Knorr et al., 2011; Dowset et al., 2013). Inspired by Fig. 5, we may think of a climate system having a higher net heat capacity  $C_p$  producing flat temperature gradients. Another argument comes from data. La Riviere et al. (2012) showed that the oceanic state in the Paleogene/Neogene had a deeper thermocline, high sea surface temperatures, and low temperature gradients. Global climate models treat ocean vertical mixing as static, although there is little reason to suspect this is correct (e.g., see Munk and Wunsch, 1998).



In order to test the effective heat capacity/mixing hypothesis, we employ the coupled climate model COSMOS which was developed at the Max-Planck Institute for Meteorology in Hamburg (Jungclaus et al., 2000). The model contains explicit diurnal and seasonal cycles, it has no flux correction and has been successfully applied to test a variety of paleoclimate hypotheses, ranging from the Miocene climate (Knorr et al., 2011; Knorr and Lohmann, 2014; Stein et al., 2016), the Pliocene (Stepanek and Lohmann, 2012) as well as glacial (Zhang et al., 2013; 2014) and interglacial climates (Wei and Lohmann, 2012; Lohmann et al., 2013; Pfeiffer and Lohmann, 2016).

Paleogene/Neogene simulations which were published so far show the underestimated flat temperature gradients as compared to data. As pointed out by Korty et al. (2008), elevated CO<sub>2</sub> is insufficient, to reduce the planetary temperature gradient to the low gradients found during equable climates (e.g., Barron and Washington, 1985; Sloan and Rea, 1996; Shellito et al., 2003). In order to mimick the effect of a higher effective heat capacity and deepened mixed layer depth, the vertical mixing coefficient is increased in the ocean, changing the values for the background vertical diffusivity by a factor of 25. The model uses a classical vertical eddy viscosity and diffusion scheme (Pacanowski and Philander, 1981). The orbital parameters are fixed to the present condition. The changed vertical mixing coefficients are mimicking possible effects like weak tidal dissipation or abyssal stratification (e.g., Green and Huber, 2013), but its explicit physics is not evaluated here.

Fig. 7 shows the anomalous near surface temperature for the new vertical mixing experiment relative to the control climate (Wei and Lohmann, 2012). Both simulations were run over 1000 years of integration in order to receive a quasi-equilibrium. The differences are related to the last 100 years of the simulation. In the vertical mixing experiment  $k_v$  was enhanced (factor of 25 is related to a  $\sim 5$  times deeper thermocline according to (14)) leading to more heat uptake by the ocean and producing equable climates with pronounced warming at polar latitudes (Fig. 7, in a similar way as in the EBM (Fig. 5). Furthermore, the model indicates that the respective winter signal of high-latitude warming is most pronounced (Fig. 7), decreasing the seasonality, also consistent with Fig. 6. The surface warming is highest at high latitudes because of the disappearance of sea ice and effective buffering of the summer heating in the surface water. Interestingly, the surface temperature distribution bears similarities with Paleogene/Neogene climate change (e.g., Wolfe, 1994; Utescher and Mosbrugger, 2007; Dowset et al., 2013). Those published temperature patterns resemble the high latitude warming (with moderate low latitude warming) structures suggesting a common mechanism in the modeled and reconstructed temperature patterns. Note, that the modelled Paleogene/Neogene warming is more intense in winter temperature than in summer temperature (Figs. 5, 7). It might be that the more effective mixing provides an explanation that high latitudes were much warmer than present and more equable in that the summer-to-winter range of temperature was much reduced (Sloan and Barron, 1990, Valdes et al., 1996; Sloan et al., 2001; Spicer et al. 2004).

There is a range of literature on the parameterisations of vertical mixing in ocean circulation models (e.g., Mellor and Yamada, 1974; Philander and Pacanowksi, 1981; Luyten et al., 1983; Large et al., 1994) and a detailed discussion is not given here. The mixing has a background value plus a mixing process strongly influenced by the shears of the mean currents. Although observations give a range of values of  $k_v$  for the ocean interior, models use simplified physics and prescribe a constant background value. In numerical modelling, the values are also constrained by the required numerical stability and to fill gaps left by other parameterisations (e.g., Griffies, 2005).  $k_v$  largely determines the intensity of the diabatic processes



and thus influence the meridional mass transport (Bryan, 1987) affecting the large-scale ocean circulation and its sensitivity (Scott and Marotzke, 2002; Prange et al., 2003; Rahmstorf et al., 2006; Green and Huber, 2013; De Boer and Hogg, 2014; de Lavergne et al., 2016; Hutchinson et al., 2018). Lambeck (1977) calculated the total rate of energy dissipation based on the numerical tide model, indicating a dominant role of ocean continent geometry and sea floor topography. Visser (2007) discussed potential biomixing in the oceans and concluded that the mixing efficiency of small organisms is extremely low. Most of the mechanical energy they impart to the oceans is dissipated almost immediately as heat. There may be a case to be made for biomixing by larger animals on a local scale, but their relatively low abundance means that they are unlikely to be important contributors to global circulation. It has to be explored if the marine organisms could have been different in the distant past in order to introduce significant changes in mixing. As a next step, one can change the large-scale ocean gateways and changed orography/topography in order to realistically simulate past climates and to separate potential forcing factors.

## 6 Conclusions

Energy balance models estimate the changes in the climate system from an analysis of the energy budget of the Earth. In their simplest form, they do not include any explicit spatial dimension, providing only globally averaged values for the computed variables. Energy balance models provide a crucial tool in climate research, especially because they - confirmed by the results of the elaborate realistic climate models - describe the processes essential for the genesis of the global climate. EBMs are thus an admissible conceptual tools, due to its reduced complexity to the essentials "scientific understanding" represents (von Storch et al., 1999). This understanding states that the radiation balance on the ground and the absorption in the atmosphere are the essential factors for determining the temperature. Eq. (3) says that the temperature is independent of the size of the Earth and the thermal characteristics, but depends on the albedo, emissivity and solar constant.

The argument follows the 1st law of thermodynamics on the conservation of energy: in steady state the Earth has to emit as much energy as it receives from the Sun. However, I argue that we shall explicitly emphasize the Earth as a rapidly rotating object with a significant heat capacity in our EBMs. Without these effects, the global mean temperature would be in the order of 163 K. The Earth system understanding says that these effects are important for the radiation balance, other processes - like horizontal transport processes - are only of secondary importance for the globally averaged temperature. The linearization of the long wave radiation in several models (North et al., 1975a, b; Chen et al., 1995) implicitly assumes the above heat capacity and fast rotation arguments. This linearization is different from the remarkable linear outgoing longwave radiation with respect to T due to the water vapor greenhouse effect (Koll and Cronin, 2018). Model scenarios in conjunction with long-term data can be used to examine mechanisms for climate change under different boundary conditions (for an overview: IPCC 2013). Ironically, the global mean in the revised EBM is very close to the original proposed value. It can be speculated that most findings dealing with climate sensitivity, the change in global temperature when changing CO<sub>2</sub>, are robust. As a basic feature, we detect the strong dependence of the temperature distribution on the effective heat capacity linked to the mixed-layer depth. A change in the mixed layer depth which likely happened through glacial-interglacial cycles (e.g. Zhang et al., 2014) is therefore an important driver constraining climate sensitivity (Köhler, et al., 2010). This could be also relevant for future



climate change when the ocean stratification can change. It would be interesting to include a temperature-dependent emissivity as e.g. in Dijkstra and Viebahn (2015).

As a key aspect for climate sensitivity, La Riviere et al. (2012) have claimed that the tight link between ocean temperature and CO<sub>2</sub> formed only during the Pliocene when the thermocline shoals and surface water became more sensitive to CO<sub>2</sub> which is therefore of major importance for the understanding of the climate-carbon cycle (Wiebe and Weaver, 1999; Zachos et al., 2008; de Boer and Hogg, 2014). Schwartz (2007) stressed out that the effective heat capacity is not an intrinsic property of the climate system but is reflective of the rate of penetration of heat energy into the ocean in response to the particular pattern of forcing and -as suggested by La Riviere et al. (2012)- also to the background state. As one application, we change the vertical mixing in the ocean affecting the effective heat capacity. The resulting temperature might explain the long-lasting question of a low equator-to-pole gradients during the Paleogene/Neogene climate (Markwick, 1994; Wolfe, 1994; Sloan and Rea, 1996; Huber et al., 2000; Shellito et al., 2003; Tripathi et al., 2003; Mosbrugger et al., 2005). It is concluded that climate studies should use improved representations of vertical mixing processes including turbulence, tidal mixing, hurricanes and wave breaking (e.g., Qiao et al., 2004; Huber et al., 2004; Simmons et al., 2004; Korty et al., 2008; Griffiths and Peltier, 2009; Green and Huber, 2013; Reichl and Hallberg, 2018). It could be that the climate models have to be de-tuned. Korty et al. (2008) explore this issue with a parameterization coupling upper tropical mixing to tropical cyclone activity. As a natural next step, one can analyze the climate-dependent heat transport due to baroclinic instability in the atmosphere (Stone and Yao, 1990; Fu et al., 1994) and ocean mixing/heat uptake (Nilsson, 1995; Munk and Wunsch, 1998; Wunsch and Ferrari, 2004; Olbers and Eden, 2017) to understand past, present and future temperatures.

*Acknowledgements.* Thanks go to Peter Köhler and Dirk Olbers for comments on earlier versions of the manuscript. Madlene Pfeiffer and Christian Stepanek are acknowledged for their contribution in producing Fig. 7. This work was funded by the Helmholtz Society through the research program PACES.

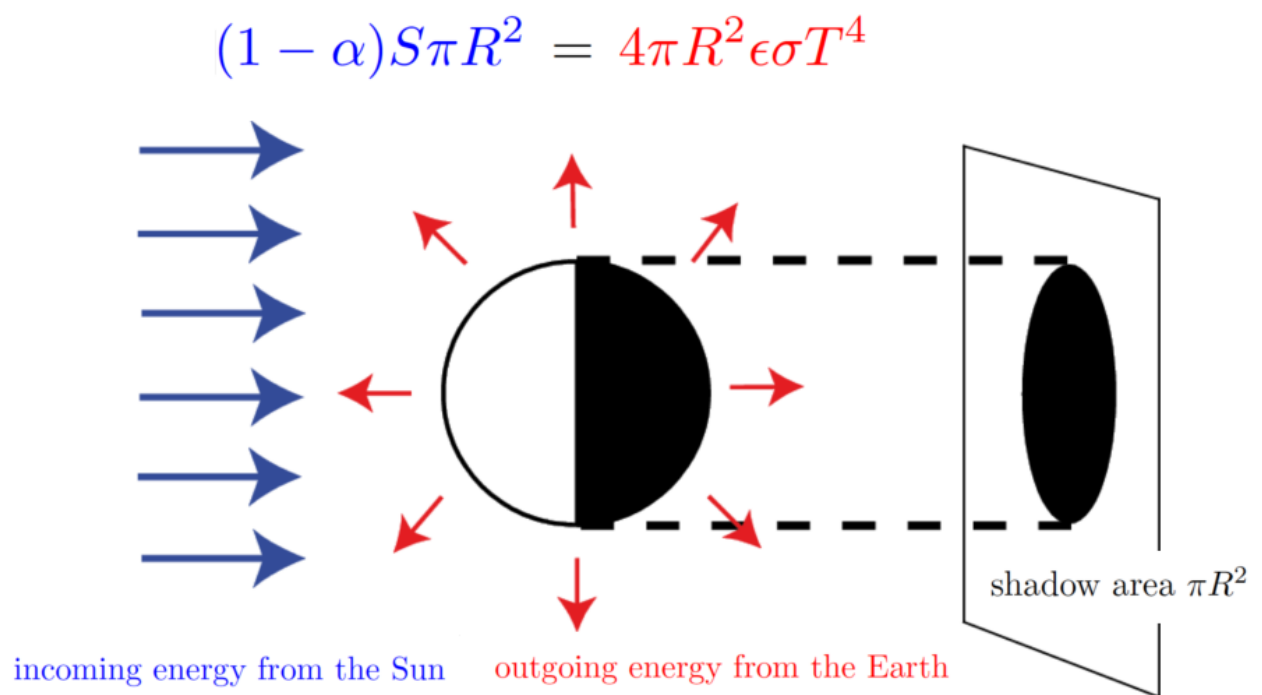


**Figure 1.** Schematic view of the energy absorbed and emitted by the Earth following (1). Modified after Goose (2015).

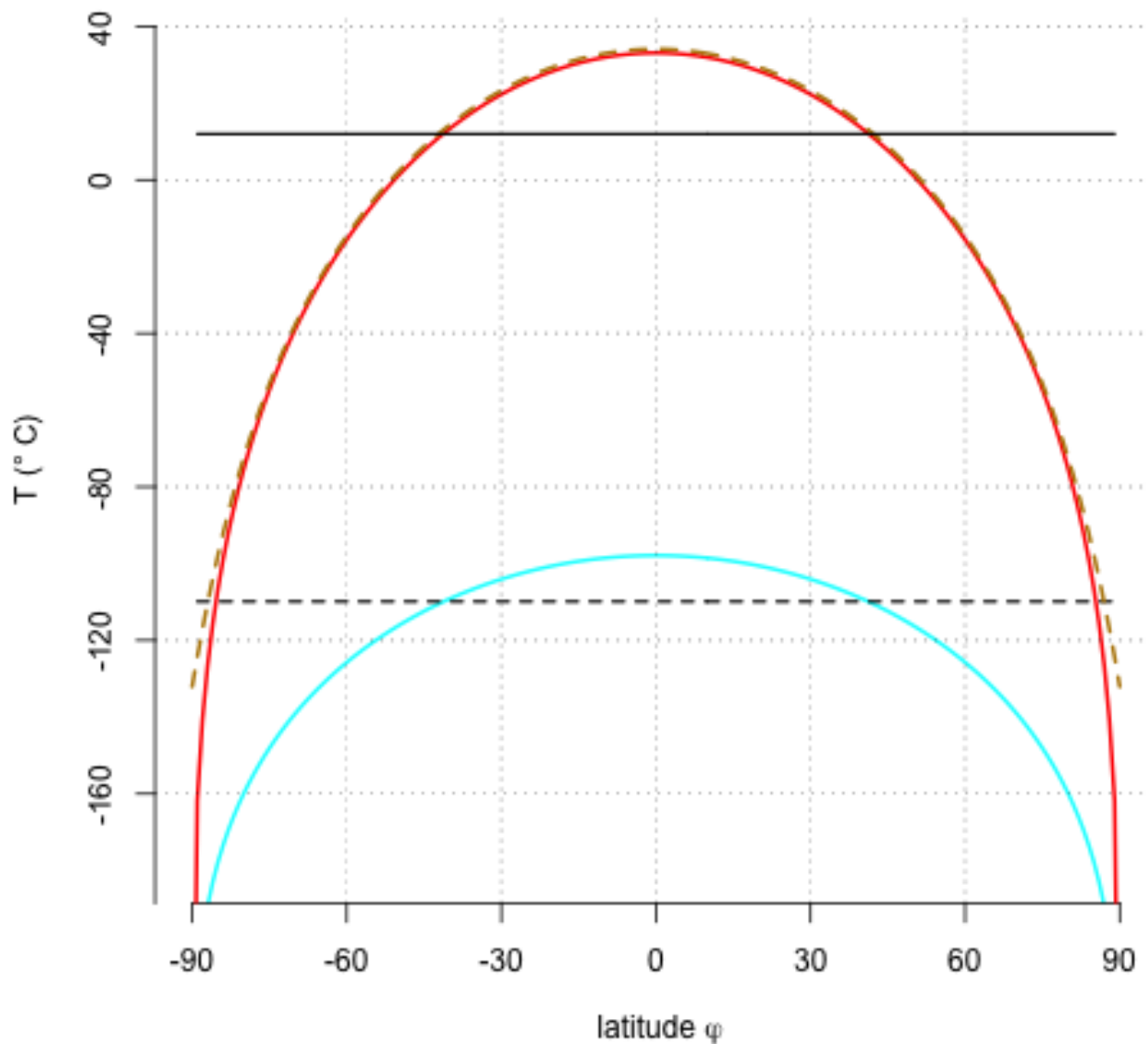


**Figure 2.** Latitudinal temperatures of the EBM with zero heat capacity (7) in cyan (its mean as a dashed line), the global approach (3) as solid black line, and the zonal and time averaging (11) in red. The dashed brownish curve shows the numerical solution by taking the zonal mean of (9).

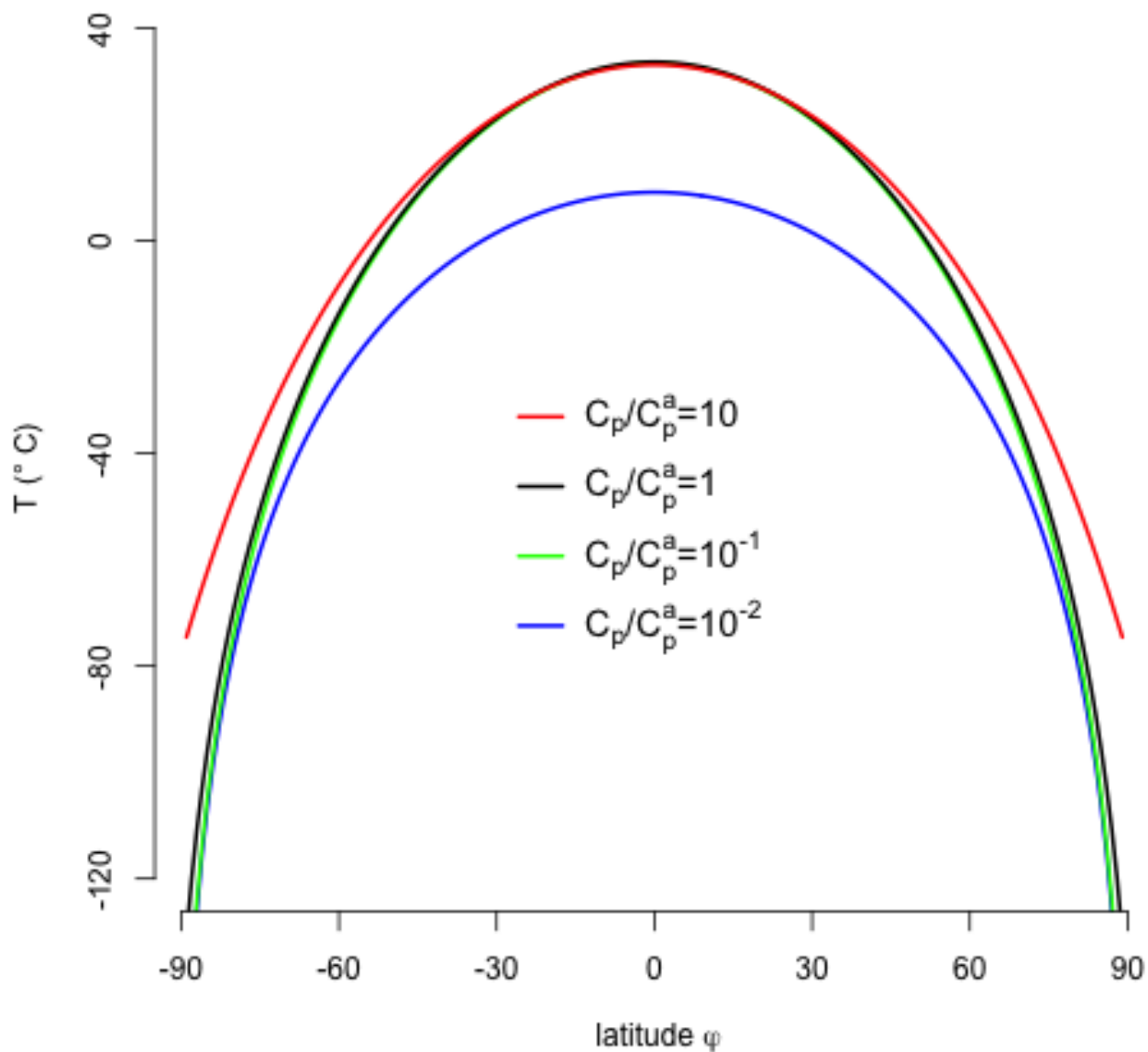


**Figure 3.** Temperature depending on  $C_p$  when solving (9) numerically. The reference heat capacity is the atmospheric heat capacity  $C_p^a = 1.02 \cdot 10^7 \text{ JK}^{-1} \text{ m}^{-2}$ . The climate is insensitive to changes in heat capacity  $C_p \in [0.05 \cdot C_p^a, 2 \cdot C_p^a]$ .

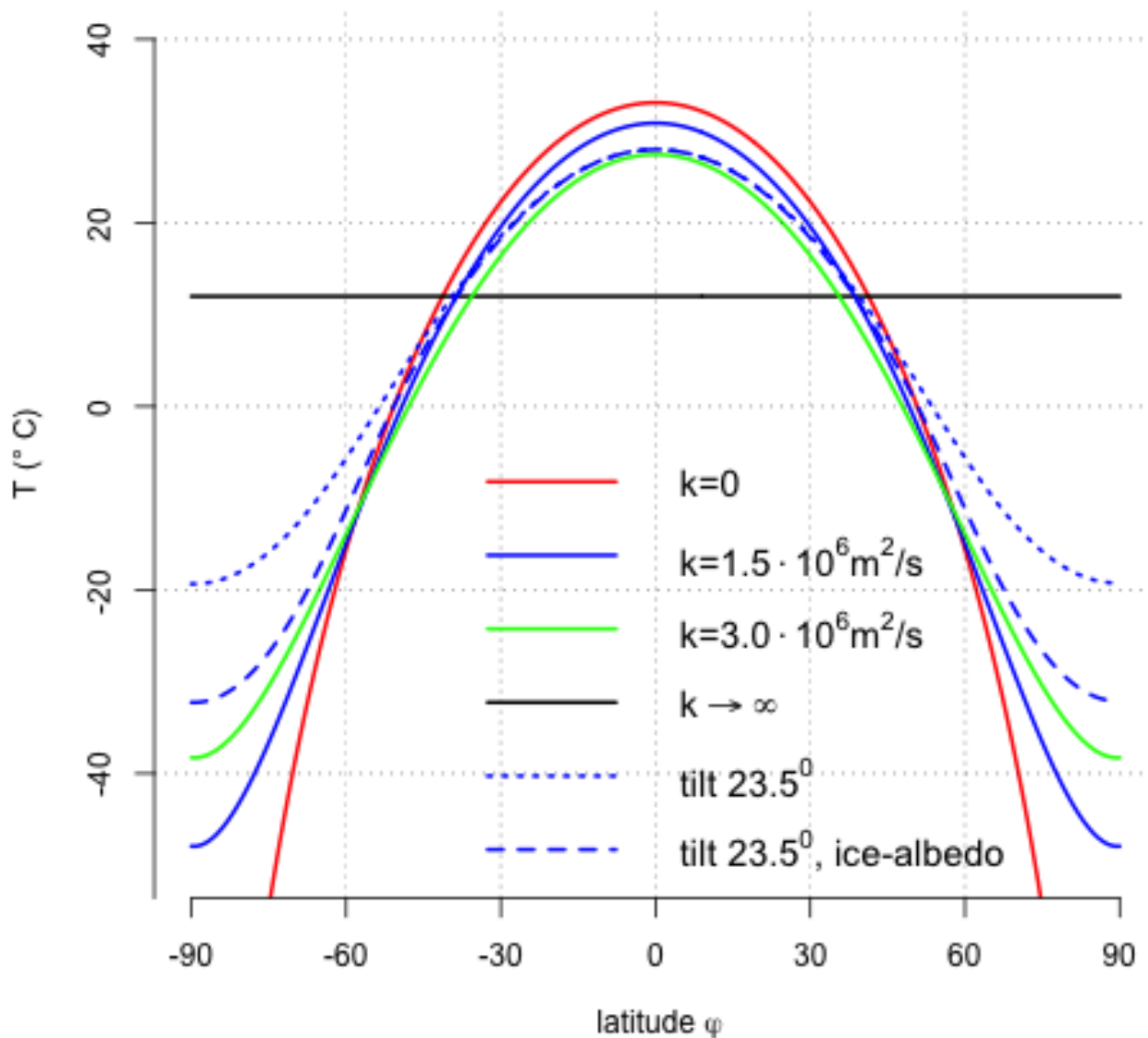


**Figure 4.** Equilibrium temperature of (15) using different diffusion coefficients.  $C_p = C_p^a$ . The blue lines use  $1.5 \cdot 10^6 \text{ m}^2/\text{s}$  with no tilt (solid line), a tilt of  $23.5^\circ$  (dotted line), and as the dashed line a tilt of  $23.5^\circ$  (present value) and ice-albedo feedback using the representation of Sellers (1969). Except for the dashed line, the global mean values are identical to the value calculated in (12). Units are  $^\circ\text{C}$ .

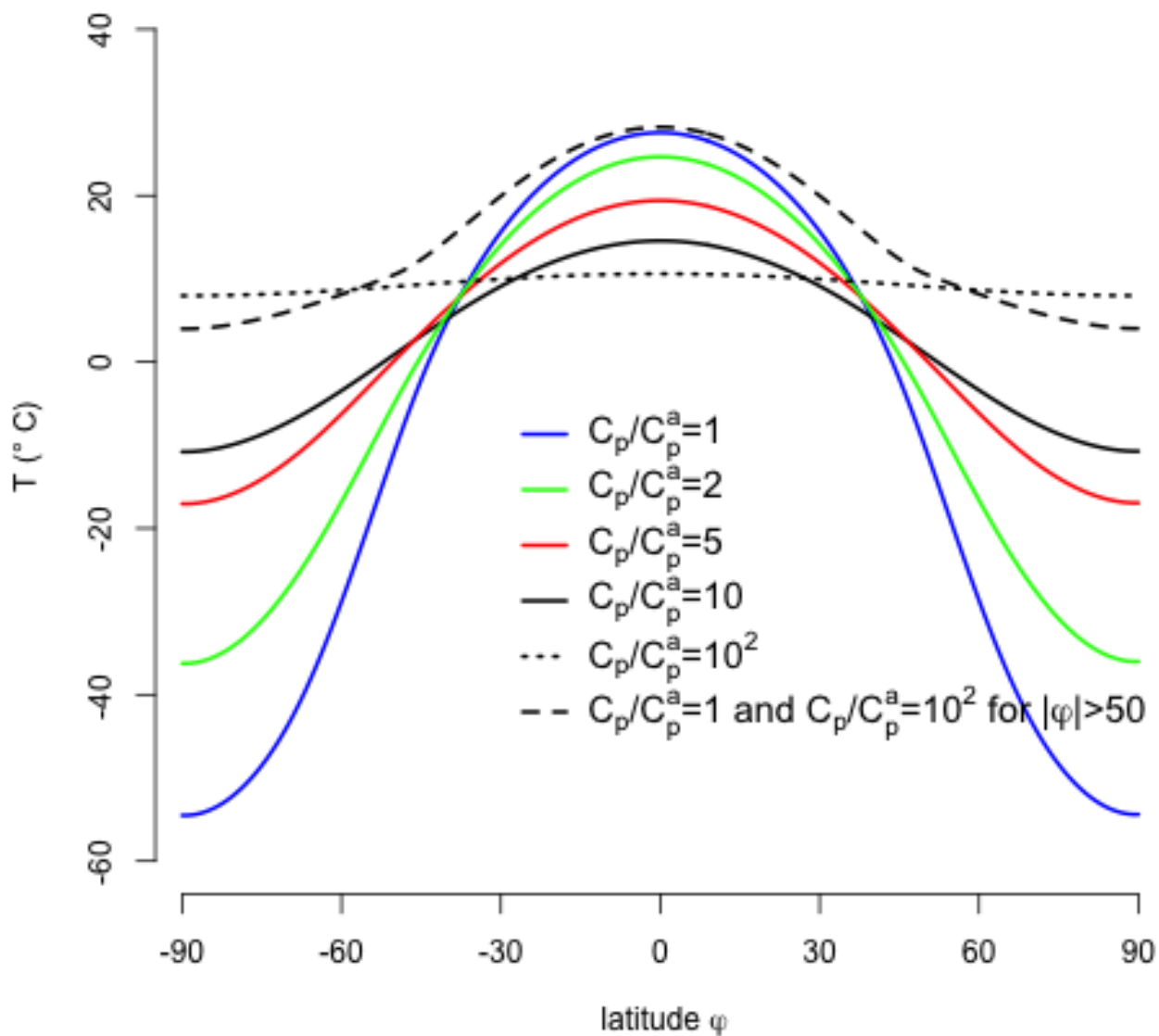


**Figure 5.** Annual mean temperature depending on  $C_p$  when solving the seasonal resolved EBM (16) numerically. For all solutions, we use  $k = 1.5 \cdot 10^6 \text{ m}^2/\text{s}$ , present day orbital parameters, and the ice-albedo feedback using the representation of Sellers (1969).

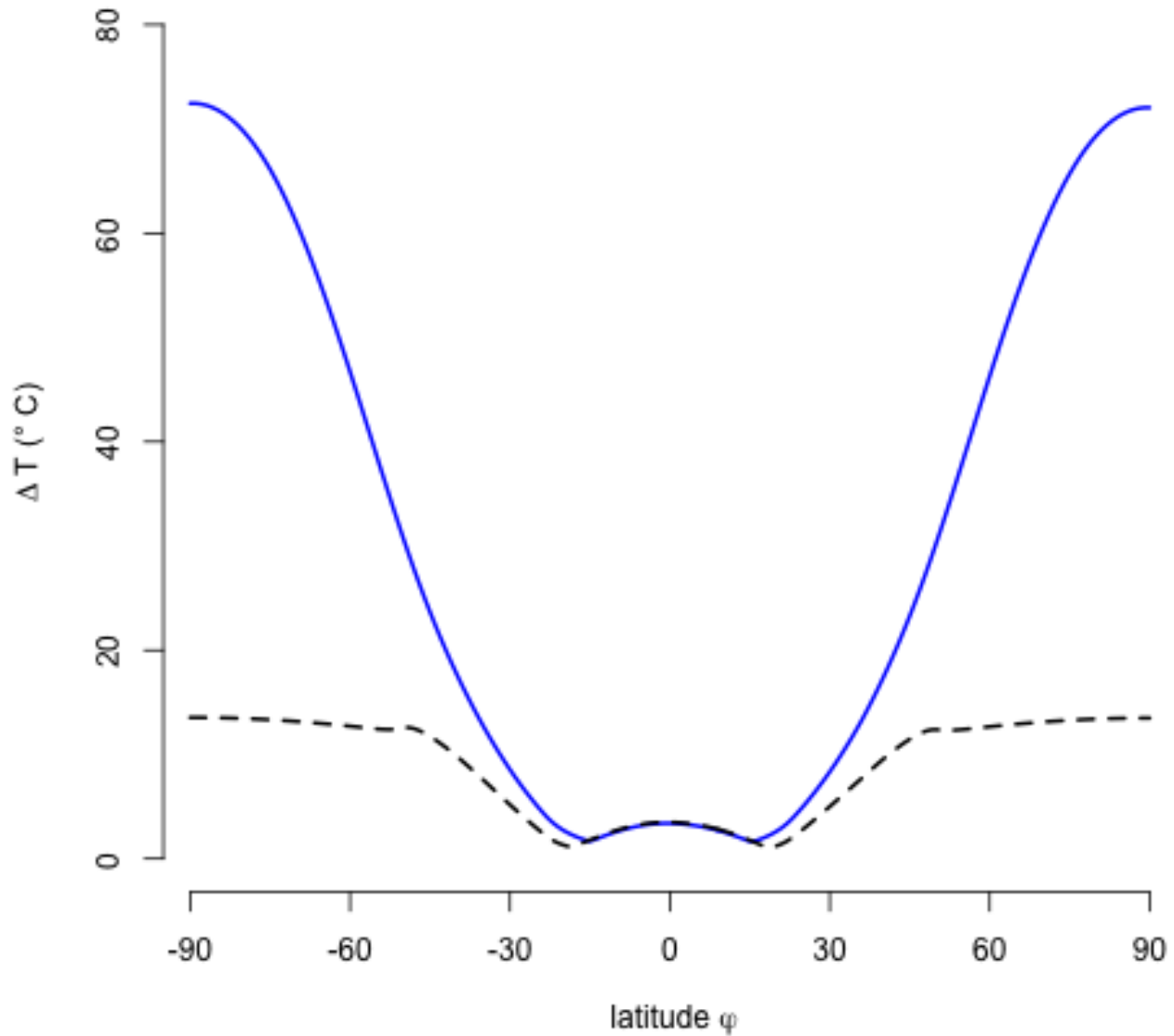


**Figure 6.** Seasonal amplitude of temperature for the two extreme scenarios in Fig. 5, indicating that a lower seasonality dashed-black relative to the blue line is linked to warmer annual mean climate.

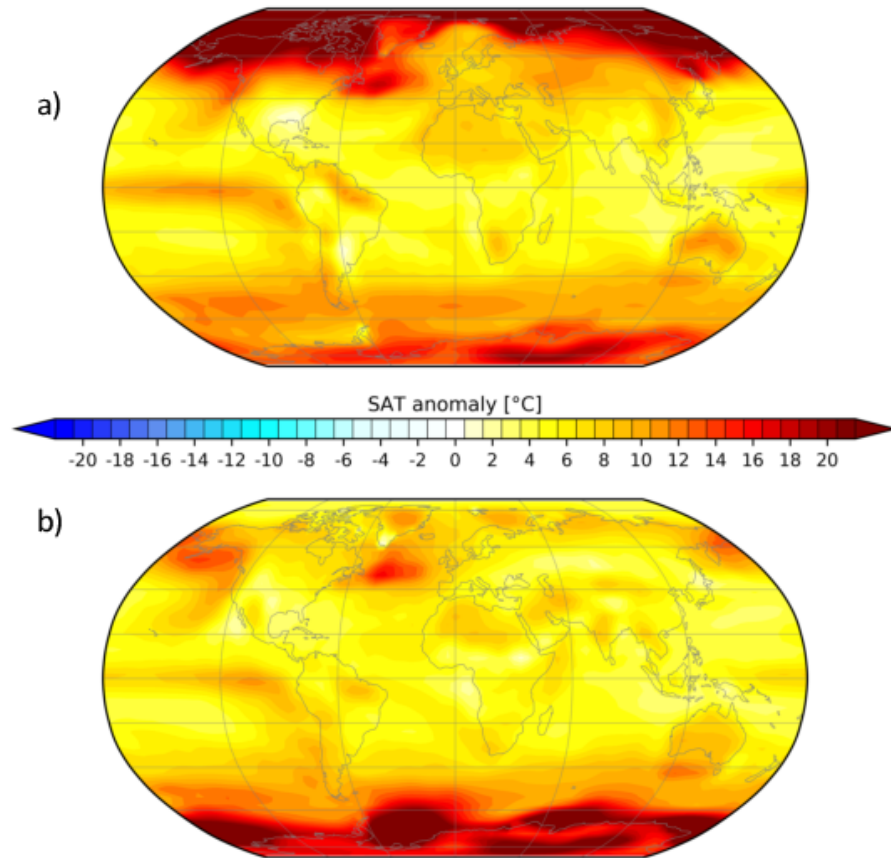


**Figure 7.** Anomalous near surface temperature for the vertical mixing experiment relative to the control climate. a) Mean over boreal winter and austral summer (DJF), b) Mean over austral winter and boreal summer (JJA). Shown is the 100 year mean after 900 years of integration using the Earth system model COSMOS. Units are °C.



## References

- Adem, J.: Experiments Aiming at Monthly and Seasonal Numerical Weather prediction. *Mon. Weather Rev.* 93,495-503, 1965.
- Adem, J.: Numerical simulation of the annual cycle of climate during the ice ages, *J. Geophys. Res.*, 86, 12015-12034, 1981.
- Anderson S.P., Weller, R.A., and Lukas, R.B.: Surface buoyancy forcing and the mixed layer of the western pacific warm pool: observations  
5 and 1D model results. *J. Clim* 9:3056-3085, 1996.
- Archer, D.: *Global Warming: Understanding the Forecast*. ISBN: 978-1-4443-0899-0. 288 pages, Wiley-Blackwell, 2009.
- Berger, A., and Loutre, M.F.: Insolation values for the climate of the last 10 million years, *Quat. Sci. Rev.*, 10(4), 297 - 317, 1991.
- Berger, A., and Loutre, M.F.: Intertropical latitudes and precessional and half-precessional cycles, *Science*, 278(5342), 1476 - 1478, 1997.
- Bryan, F.: Parameter sensitivity of primitive equation ocean general circulation models. *J. Phys. Oceanogr.* 17, 970-985, 1987.
- 10 Budyko, M.I.: The effect of solar radiation variations on the climate of the Earth. *Tellus* 21,611-619, 1969.
- Chen, D., Gerdes, R., and Lohmann, G.: A 1-D Atmospheric energy balance model developed for ocean modelling. *Theor. Appl. Climatol.*  
51, 25-38, 1995.
- Claussen, M., Mysak, L.A., Weaver, A.J., Crucifix, M., Fichefet, T., Loutre, M.-F., Weber, S.L., Alcamo, J., Alexeev, V.A., Berger, A., Calov,  
R., Ganopolski, A., Goosse, H., Lohmann, G., Lunkeit, F., Mokhov, I.I., Petoukhov, V., Stone, P., and Wang, Z.: Earth System Models of  
15 Intermediate Complexity: Closing the Gap in the Spectrum of Climate System Models. *Climate Dynamics* 18, 579-586, 2002.
- de Boer, A. M. and Hogg, A. M.: Control of the glacial carbon budget by topographically induced mixing, *Geophys. Res. Lett.*, 41, 4277-  
4284, 2014.
- Dijkstra, H.A., and Viebahn, J.P.: Sensitivity and resilience of the climate system: A conditional nonlinear optimization approach. *Communi-  
cations in Nonlinear Science and Numerical Simulation*, 22(1-3):13-22, 2015.
- 20 de Lavergne, C., Madec, G., Le Sommer, J., Nurser, A. J. G., and Naveira Garabato, A. C.: The Impact of a Variable Mixing Efficiency on  
the Abyssal Overturning, *J. Phys. Oceanogr.*, 46, 663-681, <https://doi.org/10.1175/JPO-D-14-0259.1>, 2016.
- Dowsett, H. J. , K. M. Foley, D. K. Stoll, M. A. Chandler, L. E. Sohl, M. Bentsen, B. L. Otto-Bliesner, F. J. Bragg, W.-L. Chan, C. Contoux, A.  
M. Dolan, A. M. Haywood, J. A. Jonas, A. Jost, Y. Kamae, G. Lohmann, D. J. Lunt , K. H. Nisancioglu, A. Abe-Ouchi, G. Ramstein, C. R.  
Riesselman, M. M. Robinson, N. A. Rosenbloom, U. Salzmann, C. Stepanek, S. L. Strother, H. Ueda, Q. Yan, Z. Zhang: Sea Surface Tem-  
25 perature of the mid-Piacenzian Ocean: A Data-Model Comparison. *Scientific Reports* 3; Article number: 2013; DOI:10.1038/srep02013 ,  
2013.
- Fanning, A.F., and Weaver, A. J.: An atmospheric energy-moisture balance model: Climatology, interpentadal climate change, and coupling  
to an ocean general circulation model. *J. Geophys. Res.* 101 (D10), 15111-15128, 1996.
- Fu, R., Del Genio, A.D., and Rossow, W.B.: Influence of ocean surface conditions on atmospheric vertical thermodynamic structure and deep  
30 convection. *J. Climate*, 7, 1092-1107, 1994.
- Ghil, M., and Childress, S.: *Topics in geophysical fluid dynamics: atmospheric dynamics, dynamo theory, and climate dynamics*. New York,  
NY: Springer, 1987.
- Ghil, M.: Climate stability for a Sellers-type model. *J. Atmos. Sci.*, 33, 3-20, 1976.
- Green, J.A.M., and Huber, M.: Tidal dissipation in the early Eocene and implications for ocean mixing, *Geophys. Res. Lett.*, 40, 2707-2713,  
35 doi:10.1002/grl.50510, 2013.
- Griffies, S.M.: *Fundamentals of Ocean Climate Models*. Princeton University Press, Princeton, USA. ISBN9780691118925 528 pp, 2005.



- Griffiths, S.D., and Peltier, W.R.: Modeling of Polar Ocean Tides at the Last Glacial Maximum: Amplification, Sensitivity, and Climatological Implications. *Journal of Climate* 22, 2905-2924, 2009.
- Goosse, H.: *Climate system dynamics and modelling*. Cambridge University Press, ISBN: 9781107445833, 2015.
- Hansen, J., Ruedy, R., Sato, M., and Lo, K.: Global surface temperature change. *Rev. Geophys.*, 48, RG4004, doi:10.1029/2010RG000345, 5 2010.
- Hartmann, D. L., *Global Physical Climatology*, Academic Press, 1994.
- Hasselmann, K.: Stochastic climate models. Part I, Theory. *Tellus*, 6:473–485, 1976.
- Huber, B.T., MacLeod, K.G., and Wing, S.L. (Eds.): *Warm Climates in Earth History*. Cambridge University Press, 462 pp, 2000.
- Huber, M., H. Brinkhuis, C. E. Stickley, K. Doos, A. Sluijs, J. Warnaar, G. L. Williams, and S. A. Schellenberg: Eocene circulation of the 10 Southern Ocean: Was Antarctica kept warm by subtropical waters?. *Paleoceanography*, 19, PA4026, doi:10.1029/2004PA001014, 2004.
- Hutchinson, D. K., A. M. de Boer, H. K. Coxall, R. Caballero, J. Nilsson, and M. Baatsen: Climate sensitivity and meridional overturning circulation in the late Eocene using GFDL CM2.1. *Clim. Past*, 14, 789-810, 2018.
- IPCC: *Climate Change: The Physical Science Basis*. Contribution of Working Group I to the Fifth Assessment Report of the Intergovernmental Panel on Climate Change [Stocker, T.F., D. Qin, G.-K. Plattner, M. Tignor, S.K. Allen, J. Boschung, A. Nauels, Y. Xia, V. Bex and 15 P.M. Midgley (eds.)]. Cambridge University Press, Cambridge, United Kingdom and New York, NY, USA, 1535 pp, 2013.
- Jungclauss, J. H., Lorenz, S. J., Timmreck, C., Reick, C. H., Brovkin, V., Six, K., Segschneider, J., Giorgetta, M. A., Crowley, T. J., Pongratz, J., Krivova, N. A., Vieira, L. E., Solanki, S. K., Klocke, D., Botzet, M., Esch, M., Gayler, V., Haak, H., Raddatz, T. J., Roeckner, E., Schnur, R., Widmann, H., Claussen, M., Stevens, B., and Marotzke, J.: Climate and carbon-cycle variability over the last millennium, *Clim. Past*, 6, 723-737, 2010.
- 20 Kawai, Y., and Kawamura, H.: Evaluation of the diurnal warming of sea surface temperature using satellite derived marine meteorological data. *J Oceanogr* 58:805-814, 2002.
- Knorr, G., Butzin, M., Micheels, A., and Lohmann, G.: A Warm Miocene Climate at Low Atmospheric CO<sub>2</sub> levels. *Geophysical Research Letters*, L20701, doi:10.1029/2011GL048873, 2011.
- Knorr, G., and Lohmann, G.: A warming climate during the Antarctic ice sheet growth at the Middle Miocene transition. *Nature Geoscience*, 25 7, 376-381, 2014.
- Köhler, P., Bintanja, R., Fischer, H., Joos, F., Knutti, R., Lohmann, G., and Masson-Delmotte, V.: What caused Earth's temperature variations during the last 800,000 years? Data-based evidence on radiative forcing and constraints on climate sensitivity. *Quaternary Science Reviews* 29, 129-145. doi:10.1016/j.quascirev.2009.09.026, 2010.
- Koll, D. D. B., and Cronin, J. R.: Earth's outgoing longwave radiation linear due to H<sub>2</sub>O greenhouse effect. *Proceedings National Academy of Sciences*, 115 (41) 10293-10298, 2018.
- 30 Korty, R. L, Emanuel, A. K. A., and Scott, J. R.: Tropical Cyclone-Induced Upper-Ocean Mixing and Climate: Application to Equable Climates. *J. Climate*, 21, 638-654, 2008.
- Laepple, T., and Lohmann, G.: The seasonal cycle as template for climate variability on astronomical time scales. *Paleoceanography*, 24, PA4201, doi:10.1029/2008PA001674, 2009.
- 35 Lambeck, K.: Tidal dissipation in the oceans: astronomical, geophysical and oceanographic consequences *Phil. Trans. R. Soc. Lond. A*, 287, 545-594, 1977.
- Large, W.G., McWilliams, J.C., and Doney, S.C.: Oceanic vertical mixing: a review and a model with a nonlocal boundary layer parameterization *Rev. Geophys.*, 32 (4), 363-403, 1994.



- Lemke, P.: Stochastic climate models, part 3. Application to zonally averaged energy models, *Tellus*, 29:5, 385-392, 1977.
- La Riviere, J.P., Ravelo, A.C., Crimmins, A., Dekens, P.S., Ford, H.L., Lyle, M., Wara, M.W.: Late Miocene decoupling of oceanic warmth and atmospheric carbon dioxide forcing. *Nature* 486, 97-100, 2012.
- Le Treut, H., R. Somerville, U. Cubasch, Y. Ding, C. Mauritzen, A. Mokssit, T. Peterson and M. Prather: Historical Overview of Climate Change. In: *Climate Change 2007: The Physical Science Basis. Contribution of Working Group I to the Fourth Assessment Report of the Intergovernmental Panel on Climate Change* [Solomon, S., D. Qin, M. Manning, Z. Chen, M. Marquis, K.B. Averyt, M. Tignor and H.L. Miller (eds.)]. Cambridge University Press, Cambridge, United Kingdom and New York, NY, USA, 2007.
- Lohmann, G.: ESD Ideas: The stochastic climate model shows that underestimated Holocene trends and variability represent two sides of the same coin. *Earth Syst. Dynam.* 9, 1279-1281, 2018.
- 10 Lohmann, G., Pfeiffer, M., Laepple, T., Leduc, G., and Kim, J.-H.: A model-data comparison of the Holocene global sea surface temperature evolution. *Clim. Past*, 9, 1807-1839, 2013.
- Lohmann, G., Gerdes, R., and Chen, D.: Sensitivity of the thermohaline circulation in coupled oceanic GCM-atmospheric EBM experiments. *Climate Dynamics* 12, 403-416, 1996.
- Lohmann, G., and Gerdes, R.: Sea ice effects on the Sensitivity of the Thermohaline Circulation in simplified atmosphere-ocean-sea ice  
15 models. *J. Climate* 11, 2789-2803, 1998.
- Luyten, J., Pedlosky, J., and Stommel, H.: The ventilated thermocline. *J. Phys. Oceanogr.*, 13, 292-309, 1983.
- Markwick, P.J.: 'Equability', continentality and Tertiary 'climate': the crocodilian perspective. *Geology*, 22, 613-616, 1994.
- Mellor, G. L. and Yamada, T.: A Hierarchy of Turbulence Closure Models for Planetary Boundary Layers. *Journal of Atmospheric Sciences* 31 (7), 1791-1806, 1974.
- 20 Mosbrugger, V., Utescher, T. , and D. L. Dilcher: Cenozoic continental climatic evolution of Central Europe. *Proceedings National Academy of Sciences*, 102: 14964-14969, 2005.
- Munk, W., and Wunsch, C.: Abyssal recipes II: Energetics of tidal and wind mixing. *Deep-Sea Res.*, 45, 1977-2010, 1998.
- Nilsson, J.: Energy flux from traveling hurricanes to the oceanic internal wave field. *J. Phys. Oceanogr.*, 25, 558-573, 1995.
- North, G. R.: Analytical solution of a simple climate model with diffusive heat transport. *J. Atm. Sci.* 32, 1300-1307, 1975a
- 25 North, G. R.: Theory of energy-balance climate models. *J. Atm. Sci.* 32, 2033-2043, 1997b.
- North G.R., Cahalan R.F., Coakley J.A.: Energy balance climate models. *Rev. Geophys. Space Phys.* 19, 91-121, 1981.
- North G.R., Mengel, J.G., Short D.A.: Simple energy balance model resolving the seasons and the continents: application to the astronomical theory of the ice ages. *J. Geophys. Res.* 88, 6576-6586, 1983.
- Olbers, D.J., Wenzel, M., and Willebrand, J.: The inference of North Atlantic circulation patterns from climatological hydrographic data.  
30 *Rev. Geophys.* 23(4), 313-356, 1985.
- Olbers, D., and Eden, C.: A closure for internal wave-mean flow interaction. Part II: Wave drag. *Journal of Physical Oceanography* 47 (6), 1403-1412, 2017.
- Pacanowski, R. C., and Philander, S. G. H.: Parameterization of Vertical Mixing in Numerical Models of Tropical Oceans. *J. Phys. Oceanogr.* 11, 83-89, 1981.
- 35 Peixoto, J. P., and Oort, A. H.: *Physics of Climate*, ISBN-13: 978-0883187128, ISBN-10: 0883187124, AIP Press, Springer Verlag, Berlin Heidelberg, New York, 1992.
- Pfeiffer, M., and Lohmann, G.: Greenland Ice Sheet influence on Last Interglacial climate: global sensitivity studies performed with an atmosphere-ocean general circulation model, *Clim. Past*, 12, 1313-1338, 2016.



- Pierrehumbert, R.T.: Principles of Planetary Climate. Cambridge University Press. Online ISBN: 9780511780783  
DOI:10.1017/CBO9780511780783, 2010.
- Prange, M., Lohmann, G., and A. Paul: Influence of vertical mixing on the thermohaline hysteresis: Analyses of an OGCM. *J. Phys. Oceanogr.*, 33 (8), 1707-1721, 2003.
- 5 Qiao, F., Yuan, Y., Yang, Y., Zheng, Q., Xia, C., and Ma, J.: Wave-induced mixing in the upper ocean: Distribution and application to a global ocean circulation model *Geophysical Research Letters* 31 (11), <https://doi.org/10.1029/2004GL019824>, 2004.
- Rahmstorf, S., M. Crucifix, A. Ganopolski, H. Goosse, I. Kamenkovich, R. Knutti, G. Lohmann, B. Marsh, L. A. Mysak, Z. Wang, A. Weaver, 2005: Thermohaline circulation hysteresis: a model intercomparison. *Geophys. Res. Lett.*, 32, L23605, doi:10.1029/2005GL023655.
- Reichl, B.G., and Hallberg, R.: A simplified energetics based planetary boundary layer (ePBL) approach for ocean climate simulations.  
10 *Ocean Modelling* 132, 112-129, 2018.
- Ruddiman, W.F.: *Earth's Climate: Past and Future*. W H Freeman & Co, 354 pages, ISBN-13: 978-0716737414, 2001.
- Saltzman, B.: *Dynamical Paleoclimatology: Generalized Theory of Global Climate Change*. ISBN-13: 978-0123971616, ISBN-10: 0123971616, 2001.
- Schwartz, S.E.: Heat capacity, time constant, and sensitivity of Earth's climate system. *J Geophys Res* 112: D24S05,  
15 doi:10.1029/2007JD008746, 2007.
- Scott, J. R., and Marotzke, J.: The location of diapycnal mixing and the meridional overturning circulation. *J. Phys. Oceanogr.*, 32, 3328-3345, 2002.
- Sellers, W. D.: A global climate model based on the energy balance of the earth-atmosphere system. *J. Appl. Meteorol.* 8, 392-400, 1969.
- Sellers, W. D.: A new global climate model. *J. Appl. Meteorol.* 12, 241-254, 1973.
- 20 Shellito, C. J., Sloan, L. C., and Huber, M.: Climate model sensitivity to atmospheric CO<sub>2</sub> levels in the early-middle Paleogene. *Palaeogeogr. Palaeoclimatol. Palaeoecol.*, 193, 113-123, 2003.
- Short, D. A., J. G. Mengel, T. J. Crowley, W. T. Hyde, and G. R. North: Filtering of Milankovitch Cycles by Earth's Geography. *Quaternary Research* 35, 2, 157-173, 1991.
- Simmons, H. L., Jayne, S. R., Laurent, L. C. S., and Weaver, A. J.: Tidally driven mixing in a numerical model of the ocean general  
25 circulation, *Ocean Model.*, 6, 245-263, [https://doi.org/10.1016/S1463-5003\(03\)00011-8](https://doi.org/10.1016/S1463-5003(03)00011-8), 2004.
- Sloan, L. C., and Rea, D. K.: Atmospheric carbon dioxide and early Eocene climate: A general circulation modeling sensitivity study. *Palaeogeogr. Palaeoclimatol. Palaeoecol.*, 119, 275-292, 1996.
- Sloan, L.C., and Barron, E.J.: Equable climates during Earth history *Geology*, 18, 489-492, 1990.
- Sloan, L.C., Huber, M., Crowley, T.J., Sewall, J.O., and Baum S.: Effect of sea surface temperature configuration on model simulations of  
30 equable climate in the early Eocene *Palaeogeogr. Palaeoclimatol. Palaeoecol.*, 167, 321-335, 2001.
- Spicer R.A., Herman, A.B., and Kennedy E.M.: The foliar physiognomic record of climatic conditions during dormancy: CLAMP and the cold month mean temperature *J. Geol.*, 112, 685-702, 2004.
- Stap, L. B., R. S. W. van de Wal, B. de Boer, P. Köhler, J. H. Hoencamp, G. Lohmann, E. Tuenter, and L. J. Lourens: Modeled influence of land  
ice and CO<sub>2</sub> on polar amplification and paleoclimate sensitivity during the past 5 million years. *Paleoceanography and Paleoclimatology*,  
35 33 (4), 381-394, 2018.
- Stein, R., K. Fahl, M. Schreck, G. Knorr, F. Niessen, M. Forwick, C. Gebhardt, L. Jensen, M. Kaminski, A. Kopf, J. Matthiessen, W. Jokat, and G. Lohmann: Evidence for ice-free summers in the late Miocene central Arctic Ocean. *Nature comm.* 7, 11148, doi:10.1038/ncomms11148, 2016.



- Stepanek, C., and Lohmann, G.: Modelling mid-Pliocene climate with COSMOS. *Geosci. Model Dev.*, 5, 1221-1243, 2012.
- Stocker, T.: Introduction to Climate Modelling. 182 pp. Springer-Verlag Berlin Heidelberg. doi:10.1007/978-3-642-00773-6 ISBN 978-3-642-00773-6, 2011.
- Stocker, T.F., Wright, D.G., and Mysak, L.A.: A zonally averaged, coupled ocean-atmosphere model for paleoclimate studies. *J. Climate* 5, 773-797, 1992.
- Stommel, H., Saunders, K., Simmons, W., and Cooper, J.: Observation of the diurnal thermocline. *Deep-Sea Res.*, 16, 269-284, 1969.
- Stone, P.H., and Yao, M.S.: Development of a two-dimensional zonally averaged statistical-dynamical model. Part III: The parametrisation of the eddy fluxes of heat and moisture. *J. Climate* 3,726-740, 1990.
- Stuart-Menteth, A.C., Robinson, I.S., and Challenor, P.G.: A global study of diurnal warming using satellite-derived sea surface temperature. *J Geophys Res* 108(C5):3155, 2003.
- Su, Q.H., and Hsieh, D.Y.: Stability of the Budyko climate model. *J. Atmos. Sci.*, 33, 2273-2275, 1976.
- Tripathi, A. K., Delaney, M. L., Zachos, J. C., Anderson, L. D. Kelly, D. C., and Elderfield, H.: Tropical sea-surface temperature reconstruction for the early Paleogene using Mg/Ca ratios of planktonic foraminifera. *Paleoceanography*, 18, 1101, 2003.
- Utescher, T., and Mosbrugger, V.: Eocene vegetation patterns reconstructed from plant diversity - A global perspective. *Palaeogeography, Palaeoclimatology, Palaeoecology* 247, 243-271, 2007.
- Valdes, P.J., Sellwood, B.W., and Price, G.D.: The concept of Cretaceous equability *Palaeoclim.: Data Model.*, 1, 139-158, 1996.
- Vasavada, A.R., Paige, D.A., and Wood, S.E.: Near-surface temperatures on Mercury and the Moon and the stability of polar ice deposits. *Icarus* 141, 179-93, 1999.
- von der Heydt, A.S., H.A. Dijkstra, R.S.W. van de Wal, R. Caballero, M. Crucifix, G.L. Foster, M. Huber, P. Köhler, E. Rohling, P. J. Valdes, P. Ashwin, S. Bathiany, T. Berends, L. G. J. van Bree, P. Ditlevsen, M. Ghil, A. Haywood, J. Katzav, G. Lohmann, J. Lohmann, V. Lucarini, A. Marzocchi, H. Pälike, I.R. Baroni, D. Simon, A. Sluijs, L.B. Stap, A. Tantet, J. Viebahn, M. Ziegler: Lessons on climate sensitivity from past climate changes. *Current Climate Change Reports* 2, 148-158. DOI:10.1007/s40641-016-0049-3, 2016.
- von Storch, H., Güss, G. S., and Heimann, M.: *Das Klimasystem und seine Modellierung: eine Einführung.* (in German) Springer-Verlag Berlin Heidelberg. 256pp. doi:10.1007/978-3-642-58528-9, 1999.
- Visser, A. W.: Biomixing of the Oceans? *Science* 316, 5826, 838-839. DOI:10.1126/science.1141272, 2007.
- Ward, B.: Near-surface ocean temperature. *J Geophys Res* 111(C5):1-18. doi:10.1029/2004JC002689, 2006.
- Wei, W., and Lohmann, G.: Simulated Atlantic Multidecadal Oscillation during the Holocene. *J. Climate*, 25, 6989-7002, 2012.
- Wiebe, E.C., and Weaver, A. J.: On the sensitivity of global warming experiments to the parameterisation of sub-grid scale ocean mixing. *Climate Dyn.*, 15, 875-893, 1999.
- Wolfe, J.A.: Tertiary climatic changes at middle latitudes of western North America. *Palaeogeography, Palaeoclimatology, Palaeoecology* 108, 195-205, 1994.
- Wunsch, C., and Ferrari, R.: Vertical mixing, energy, and the general circulation of the oceans. *Annu. Rev. Fluid Mech.* 36:281-314, 2004.
- Zachos, J.C., Dickens, G.R., and Zeebe, R.E.: An early Cenozoic perspective on greenhouse warming and carbon-cycle dynamics. *Nature*, 451, 279-283, 2008.
- Zhang, X., Lohmann, G., Knorr, G., and Xu, X.: Different ocean states and transient characteristics in Last Glacial Maximum simulations and implications for deglaciation. *Clim. Past*, 9, 2319-2333, 2013.
- Zhang, X., Lohmann, G., Knorr, G., and Purcell, C.: Abrupt glacial climate shifts controlled by ice sheet changes. *Nature* 512, 290-294, 2014.